



This is the accepted manuscript made available via CHORUS. The article has been published as:

Open inflation in the landscape

Daisuke Yamauchi, Andrei Linde, Atsushi Naruko, Misao Sasaki, and Takahiro Tanaka

Phys. Rev. D **84**, 043513 — Published 10 August 2011

DOI: [10.1103/PhysRevD.84.043513](https://doi.org/10.1103/PhysRevD.84.043513)

Open inflation in the landscape

Daisuke Yamauchi^{1,2,*}, Andrei Linde^{3,†}, Atsushi Naruko^{1,‡}, Misao Sasaki^{1,§} and Takahiro Tanaka^{1,¶}

¹*Yukawa Institute for Theoretical Physics, Kyoto University, Kyoto, Japan*

²*Institute for Cosmic Ray Research, The University of Tokyo, Kashiwa 277-8582, Japan*

³*Department of Physics, Stanford University, Stanford, CA 94305-4060, USA*

Open inflation scenario is attracting a renewed interest in the context of string landscape. Since there are a large number of metastable de Sitter vacua in string landscape, tunneling transitions to lower metastable vacua through the bubble nucleation occur quite naturally, which leads to a natural realization of open inflation. Although the deviation of Ω_0 from unity is small by the observational bound, we argue that the effect of this small deviation on the large angle CMB anisotropies can be significant for tensor-type perturbation in open inflation scenario. We consider the situation in which there is a large hierarchy between the energy scale of the quantum tunneling and that of the slow-roll inflation in the nucleated bubble. If the potential just after tunneling is steep enough, a rapid-roll phase appears before the slow-roll inflation. In this case the power spectrum is basically determined by the Hubble rate during the slow-roll inflation. On the other hand, if such rapid-roll phase is absent, the power spectrum keeps the memory of the high energy density there in the large angular components. Furthermore, the amplitude of large angular components can be enhanced due to the effects of the wall fluctuation mode if the bubble wall tension is small. Therefore, although even the dominant quadrupole component is suppressed by the factor $(1 - \Omega_0)^2$, one can construct some models in which the deviation of Ω_0 from unity is large enough to produce measurable effects. We also consider a more general class of models, where the false vacuum decay may occur due to Hawking-Moss tunneling, as well as the models involving more than one scalar field. We discuss scalar perturbations in these models and point out that a large set of such models is already ruled out by observational data, unless there was a very long stage of slow-roll inflation after the tunneling. These results show that observational data allow us to test various assumptions concerning the structure of the string theory potentials and the duration of the last stage of inflation.

PACS numbers: Valid PACS appear here

I. INTRODUCTION

The recent observational data show that the universe is almost exactly flat, $\Omega_0 = 1$ with accuracy of about 1% [1]. This result is in an excellent agreement with the predictions of the simplest inflationary models [2]. However, in the context of string landscape scenario [3–5] it is quite possible that our part of the universe appeared as a result of quantum tunneling, after being trapped in one of the many metastable vacua of string theory. In many cases, tunneling can be described by an Euclidean $O(4)$ -symmetric bounce solution called Coleman-De Luccia (CDL) instanton [6, 7]. Due to the symmetry of the bounce solution, the expanding bubble has $O(3, 1)$ symmetry. The bubble formed by the CDL instanton looks from the inside like an infinite open universe [6, 7]. If there was no inflation after tunneling, the interior of the bubble becomes an almost empty curvature dominated universe with $\Omega_0 \ll 1$, which is ruled out by observations. However, if the universe experienced a sufficiently long stage of slow-roll inflation inside the light-cone ema-

nating from the center of the bubble, the universe almost exactly flat, with $\Omega_0 \approx 1$ [8–16].

If inflation inside the bubble is too long, the universe will be absolutely flat, and hence we would be unable to tell whether our part of the universe was produced by this mechanism. Therefore one could argue that it would require significant fine-tuning to produce an open universe with a minuscule but still observable deviation of Ω_0 from 1, e.g. $1 - \Omega_0 \sim 10^{-2} - 10^{-3}$. However, this conclusion is not necessarily correct. Freivogel et al. argued that long stage of inflation in string theory may be improbable, so it would be natural to have $\Omega_0 \ll 1$ [17]. The only reason why we do not live in such a universe is that formation of galaxies would be disrupted by expansion of a curvature dominated open universe, just as it is disrupted by the existence of a cosmological constant [18]. This provides a possible anthropic explanation of the smallness of the parameter $1 - \Omega_0$. According to [17], the probability to observe the deviation from flatness $1 - \Omega_0 < 0.02$ is about 90%. This result was further strengthened in [19], where it was shown that in a certain class of the probability measures, the probability to find a universe with $1 - \Omega_0 > 10^{-3}$ is only about 6%. One should bear in mind that such estimates strongly depend on the choice of the probability measure, which remains an unsolved problem. However, these estimates suggest that one can obtain an explanation of the observed flatness of the universe compatible with a relatively short stage of slow-roll inflation inside an open universe. Therefore, it is not

*Electronic address: yamauchi@icrr.u-tokyo.ac.jp

†Electronic address: alinde@stanford.edu

‡Electronic address: naruko@yukawa.kyoto-u.ac.jp

§Electronic address: misao@yukawa.kyoto-u.ac.jp

¶Electronic address: tanaka@yukawa.kyoto-u.ac.jp

very improbable that $1 - \Omega_0$ may be in the observable range. The goal of our paper is to study possible observational consequences of the open universe scenario with $1 - \Omega_0 \sim 10^{-2} - 10^{-3}$ for the Cosmic Microwave Background (CMB) anisotropy. We will focus on tensor perturbations.

One should note that even though the basic idea of this scenario is pretty simple, it is not easy to find a realistic open inflation model in the single field inflationary scenario. For example, the simplest potential which allows inflation at $\phi > M_{\text{pl}}$ and has a metastable vacuum state at large ϕ can be written as a sum $m^2\phi^2/2 - \delta\phi^3/3 + \lambda\phi^4/4$, where $m^2, \delta, \lambda > 0$. An investigation of inflation in this scenario demonstrated that $V'' < H^2$ in the vicinity of the barrier [20]. In this case the tunneling occurs not through the barrier, but to the top of the barrier, described by the so-called Hawking-Moss instanton [21–25]. Then we will have eternal inflation at the top of the barrier with $V' = 0$, $V'' < H^2$, which leads to generation of density perturbations $O(1)$ on the curvature scale. Therefore if the subsequent stage of the slow-roll inflation is short, we would see enormously large CMB perturbations on the horizon. This would dramatically contradict the results of the cosmological observations, unless the subsequent stage of inflation is very long, which makes the universe flat, $\Omega = 1$.

It is possible to overcome this problem and find single-field models where CDL instantons lead to tunneling and subsequent inflation. Up to now, only one explicit model of this type was proposed [26, 27], but the inflaton potential of this model is quite complicated. The scalar perturbations ignoring the self-gravity of these fluctuations in single-field models has been considered in [10–16]. As for the tensor perturbations, the studies in which the perturbation of scalar field was neglected was done in [28–31]. The general formula for the power spectrum for the single-field open inflation was given in [32, 33].

It is much simpler to construct models with two fields, where the stage of the slow-roll governed by one of the fields is synchronized by the tunneling of another field, see e.g. [20, 34–41]. However, synchronization of the tunneling in these models is only approximate. Therefore the geometry of the universe inside the bubble is not exactly described by the metric of an open homogeneous universe. That is why these models were called “quasi-open” [20].

In the simplest models of this type, the universe inside the bubble has an island-like structure, since a sufficiently large number of e-folds is possible only around the maximum of density formed by the statistical fluctuation. If we consider the simplest possibility that there is no direct interaction between the tunneling field and the inflaton field that drives inflation inside the bubble, these models are troubled with large supercurvature perturbations, especially when the energy scales before and after tunneling are significantly different. The angular power spectrum for the supercurvature perturbations are esti-

mated as [34, 35, 41] (see also [14])

$$\frac{\ell(\ell+1)}{2\pi} C_\ell^{(\Lambda)} \approx \frac{\kappa}{\epsilon_{\text{inf}}} \left(\frac{H_L}{2\pi} \right)^2 (1 - \Omega_0)^\ell,$$

where $\kappa = 1/M_{\text{pl}}^2 = 8\pi G$, H_L is the Hubble rate on the false vacuum side, and ϵ_{inf} denotes the slow-roll parameter during the standard slow-roll inflation. (In the following, we often use the Planck units in which M_{pl} is set to unity.) This amplitude of fluctuation has steep ℓ dependence and is much larger than the ordinary slow-roll power spectrum determined by the Hubble rate during the open inflation unless $1 - \Omega_0$ is extremely small. Therefore we need to introduce some complications even in two field models, in order to make them compatible with observations [35].

Originally, the models of open inflation were proposed in order to describe an inflationary universe with $\Omega_0 \sim 0.3$. The possibility that $\Omega_0 \sim 0.3$ were eventually ruled out from the CMB observations, but CMB observations do not rule out the possibility that inflation after tunneling is sufficiently long and Ω_0 is sufficiently close to 1. This fact gives a revived interest in the generation of perturbation in these models from the point of view of testing some of the predictions of the string landscape scenario. Indeed, we will find that some models based on CDL tunneling are consistent with the existing observational data for $1 - \Omega_0 \sim 10^{-3}$, but may be ruled out for $1 - \Omega_0 \sim 10^{-2}$. Furthermore, models of quasiopen inflation, as well as the models leading to the Hawking-Moss tunneling [21, 23, 24], may lead to very specific predictions, which may allow us to test basic principles of the string inflation scenario and to study observational consequences of the decay of the metastable string theory vacua. The general requirement to this class of model is that $1 - \Omega_0$ must be extremely small, which means that inflation after the tunneling must be very long.

The models to be studied in this paper will be quite generic, but we will keep in mind some of the expected features of tunneling in the landscape and the last stage of the slow-roll inflation. In particular, a typical vacuum energy in the landscape can approach Planck density or density close to the scale of the grand unification, even though of course there are many vacua with much smaller energy density. Meanwhile, in many models of slow-roll inflation based on the KKLT scenario of stabilization of stringy vacua [3], the maximal Hubble constant at the last stage of the slow-roll inflation cannot be greater than the gravitino mass [42]. In such models, the typical vacuum energy of the decaying metastable vacuum in the open universe scenario is many orders of magnitude greater than the energy density during the last stage of the slow roll inflation.

In this paper we will concentrate on the investigation of the models with the CDL tunneling and investigate the CMB temperature fluctuations. We will focus on tensor perturbations since tensor perturbations are more sensitive to the value of the Hubble parameter and properties of tunneling than scalar perturbations. In the end

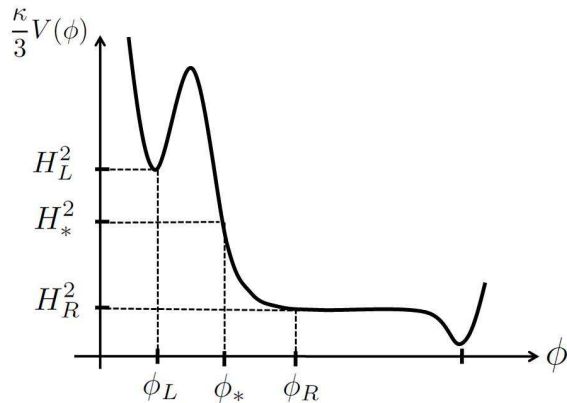


FIG. 1: Schematic picture of the effective potential for inflation in one-bubble open inflation scenario.

of the paper we will briefly discuss scalar perturbations and their cosmological implications.

This paper is organized as follow. In Sec. II we describe the background evolution of the models of open inflation in the context of the string landscape scenario. There we introduce models with a rapid roll phase after the bubble nucleation. In Sec. III we first review the method to evaluate the tensor perturbation after the false vacuum decay, and apply it to our models to identify the typical signature in the CMB spectrum. Section IV is devoted to summary.

II. BACKGROUND EVOLUTION OF THE OPEN INFLATION MODELS IN THE LANDSCAPE

A. Bubble nucleation

The system which we are going to consider consists of a minimally coupled scalar field, ϕ with Einstein gravity. As we mentioned in Sec I, the most important cosmological consequence in string landscape was that there was a tunneling event in our past. Let us consider an effective potential $V(\phi)$ with a local minimum at ϕ_L , a slow-roll inflationary plateau at ϕ_R and a point where the field emerges at ϕ_* , as shown in Fig. 1. The action is given by

$$S = \int \sqrt{-g} d^4x \left[\frac{1}{2\kappa} R - \frac{1}{2} g^{\mu\nu} \partial_\mu \phi \partial_\nu \phi - V(\phi) \right]. \quad (1)$$

In this paper, we assume that the final tunneling transition occurs through CDL instanton. Let us consider the $O(4)$ -symmetric bounce solution [6, 7]. An $O(4)$ -symmetric bubble nucleation is described by the Euclidean solution (instanton). The metric is given by

$$ds^2 = dt_E^2 + a_E^2(t_E) (d\chi_E^2 + \sin^2 \chi_E d\Omega^2), \quad (2)$$

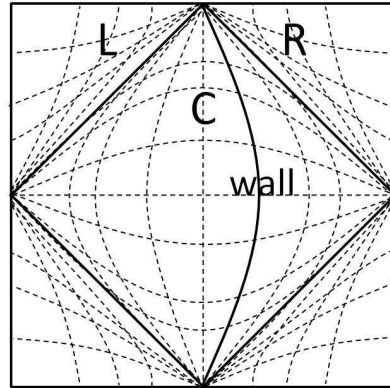


FIG. 2: The Penrose diagram for the bubble nucleating universe when the inside of the bubble terminates in a de Sitter vacuum.

and the background scalar field is denoted by $\phi = \phi(t_E)$.

The Euclidean background equations are given by

$$\left(\frac{\dot{a}_E}{a_E} \right)^2 - \frac{1}{a_E^2} = \frac{\kappa}{3} \left(\frac{1}{2} \dot{\phi}^2 - V(\phi) \right), \quad (3)$$

$$\left(\frac{\dot{a}_E}{a_E} \right)' + \frac{1}{a_E^2} = -\frac{\kappa}{2} \dot{\phi}^2, \quad (4)$$

$$\ddot{\phi} + 3 \frac{\dot{a}_E}{a_E} \dot{\phi} - V'(\phi) = 0, \quad (5)$$

where a dot represents differentiation with respect to t_E .

The background geometry and the field configuration in the Lorentzian regime are obtained by the analytic continuation of the bounce solution. It is convenience to use the coordinate η defined by $dt = a(\eta)d\eta$. The coordinates in the Lorentzian regime are given by (see e.g. [13, 34])

$$\eta_E = \eta_C = -\eta_R - \frac{\pi}{2}i = \eta_L + \frac{\pi}{2}i, \quad (6)$$

$$\chi_E = -i\chi_C + \frac{\pi}{2} = -i\chi_R = -i\chi_L, \quad (7)$$

$$a_E = a_C = ia_R = ia_L. \quad (8)$$

The Penrose diagram for this open FRW universe is presented in Fig. 2.

Typically, CDL instantons exist only if $V'' > \kappa V$ [22]. This condition, in combination with the requirement of the subsequent long stage of the slow-roll inflation, requires a very special choice of potentials in the single-field models [26, 27]. Alternatively, one may consider multi-field models [20, 35–37, 40].

In this paper, we will concentrate on the single-field models and assume that the CDL instanton exists. Meanwhile, inflation typically requires $V'' \ll \kappa V$. It is difficult to make these two conditions compatible. Therefore one may expect that the slow-roll inflation

does not start immediately after the CDL tunneling, and there must be some intermediate stage of rapid rolling down [26, 27].

This intermediate regime may last for a long time if the field potential is steep after tunneling. In general, this may be a typical situation during the tunneling in the string landscape scenario. As we mentioned in the introduction, the tunneling in the landscape may occur from a metastable vacuum with a very high value of energy density. Unless we have some specific knowledge about this vacuum state, one may assume that the scale of the energy density of this vacuum may be $O(1)$ in Planck units, or it may take some value on the grand unification energy scale $\sim 10^{-10}$. Meanwhile in many models of the slow-roll inflation based on string theory with vacuum stabilization, the Hubble constant must be smaller than the gravitino mass [42]. Although it is possible to avoid this conclusion, it is very hard to do it without fine-tuning. If the gravitino mass is of the order 1 TeV or lower, the corresponding vacuum energy density during the last stage of the slow-roll inflation should be smaller than 10^{-30} , in Planck units.

Our knowledge of the string landscape is very incomplete, so one should not fully rely on the estimates given above. However, on the basis of our present understanding of the situation, one should not be surprised to have a very long-lasting non-inflationary stage after tunneling, which should last until the large energy density of the metastable vacuum state is reduced by many orders of magnitude and the slow-roll inflation begins. We will show that the behavior in the phase of the rapid rolling down significantly affects the CMB power spectrum. In the next subsection, we will investigate the field evolution inside the open universe in the region R in Fig. 2.

B. Inflation in the open universe

In order to study the field dynamics inside the light-cone emanating from the center of the bubble (region R), it is useful to use the following identity:

$$\frac{d \ln \rho_\phi}{d \ln a_R} = -3(1 + w_\phi), \quad (9)$$

where $\rho_\phi = \dot{\phi}^2/2 + V$, $p_\phi = \dot{\phi}^2/2 - V$ and $w_\phi \equiv p_\phi/\rho_\phi$. The asymptotic boundary conditions at the nucleation point are given by

$$a_R(t) = t, \quad \dot{\phi}(t) = -\frac{V'(\phi_*)}{4}t. \quad (10)$$

Thus, we have

$$1 + w_\phi = \mathcal{O}\left(\frac{\dot{\phi}^2}{V}\right) = \mathcal{O}(\epsilon_* H_*^2 t^2). \quad (11)$$

where we have introduced

$$\epsilon \equiv \frac{1}{2\kappa} \left(\frac{V'}{V} \right)^2, \quad (12)$$

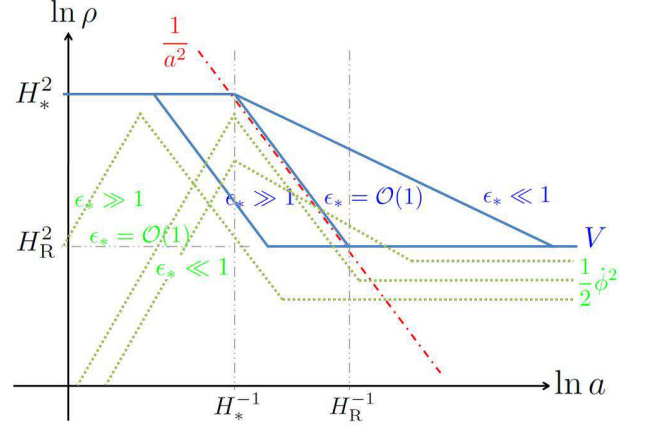


FIG. 3: A schematic picture of the evolution of the spatial curvature term (the dotted line in red), the kinetic term of the field (the solid curves in blue) and the potential term of the field (the dot-dashed curves in green).

and $\epsilon_* = \epsilon(\phi_*)$. We have also introduced $H_*^2 \equiv \kappa V(\phi_*)/3$, which is not the expansion rate at $t = 0$. This suppressed decrease rate of the energy density at around $t = 0$ is caused by the large Hubble friction due to the spatial curvature term. Hence, the field at $t \approx 0$ rolls slowly even if the potential is steep. As the spatial curvature term decays, eventually the potential energy starts to dominate or the energy density starts to decay. The potential dominance starts at $t \approx H_*^{-1}$ while the decay of the energy density starts when $1 + w_\phi$ becomes $O(1)$, i.e. at $t \approx \epsilon_*^{-1/2} H_*^{-1}$. Thus, the scenario changes depending on whether ϵ_* is large or small compared with unity. It is shown in Fig. 3 schematically how the evolution of the energy density depends on ϵ_* , assuming that ϵ stays constant until the field falls down to a plateau of the potential.

First, we consider the case with $\epsilon_* \ll 1$. In this case potential energy starts to dominate at $t \approx H_*^{-1}$ after a short curvature dominated stage, and there is no rapid roll regime. Once the potential term dominates, $1 + w_\phi$ becomes $O(\epsilon)$ as usual. Then, the energy density of the field decays slowly unless the potential becomes steep again at a later stage.

In contrast, if the potential is steep at the nucleation point, i.e. $\epsilon_* \geq 1$, the situation is different. As one can see from Eq. (11), $1 + w_\phi$ becomes $O(1)$ at $t \approx \epsilon_*^{-1/2} H_*^{-1}$ before the potential starts to dominate. The energy density of the field starts to decay rapidly proportional to $a_R^{-3(1+w_\phi)}$. During this rapid roll phase, $1 + w_\phi$ is estimated as

$$1 + w_\phi = \mathcal{O}\left(\epsilon \frac{\kappa V}{H^2}\right). \quad (13)$$

where we have used $\dot{\phi} = \mathcal{O}(V'/H)$. One can see that the rapid roll phase lasts as far as $\epsilon \gg H^2/\kappa V (\gtrsim 1)$.

When the field falls down to a plateau of the potential, the velocity of the field eventually decreases. Then, the slow-roll inflation starts and the curvature term becomes completely irrelevant for the background expansion of the universe. We denote the Hubble parameter at the onset of this slow-roll phase by H_R .

An interesting feature of the dynamics for a steep slope is “tracking”, which means that the ratios among the kinetic term, the potential term and the curvature term are approximately constant. Suppose $\epsilon(\phi)$ is a constant for simplicity. This is exactly realized when the potential is exponential-type:

$$\frac{\kappa}{3}V(\phi) = H_*^2 \exp\left[\sqrt{2\kappa\epsilon_*}(\phi - \phi_*)\right]. \quad (14)$$

To see that an exact tracking solution exists in this case, we solve Eqs. (3), (4) and (5) under the assumption

$$\phi(t) \propto \ln t. \quad (15)$$

Only if $\epsilon_* > 1$, one can solve these equations consistently to find

$$a_{R,\text{track}}(t) = \frac{t}{\sqrt{1 - 1/\epsilon_*}}, \quad (16)$$

$$\phi_{\text{track}}(t) = \phi_* + \sqrt{\frac{2}{\kappa\epsilon_*}} \ln\left[\sqrt{\frac{3}{2}}\epsilon_* H_* t\right]. \quad (17)$$

It is obvious that the above solution is an exactly tracking solution. Furthermore, one can show that it is an attractor solution.

We should note that the tracking occurs even for $\epsilon_* = \mathcal{O}(1)$. The difference from the case with $\epsilon_* \gg 1$ is that the curvature term is subdominant for the expansion of the universe in this case during the tracking phase. This means that the curvature length is well outside the horizon scale for $\epsilon_* = \mathcal{O}(1)$, while it remains comparable to the horizon scale for $\epsilon_* \gg 1$.

The above simplest example does not have a transition to the late-time slow-roll phase. Here we introduce two simple toy models, which have the transition from the initial rapid roll phase to the late-time slow-roll phase, and we discuss the tensor perturbation in these models later.

The first model has the effective potential of the following type:

$$\frac{\kappa}{3}V(\phi) = (H_*^2 - H_R^2) \exp\left[\sqrt{2\kappa\epsilon_*}(\phi - \phi_*)\right] + H_R^2, \quad (18)$$

with $H_* \gg H_R$. The potential of a similar-type often appears in supergravity and superstring theory. As a concrete example, we will choose the parameters like $H_*^2 = 10^{-3}M_{\text{pl}}^2$, $H_R^2 = 10^{-30}M_{\text{pl}}^2$ and $\phi_* = 10M_{\text{pl}}$. In Fig. 4, the time evolution of the energy densities for $\epsilon_* = 0.1, 0.5, 1, 10^2$ and 10^4 is shown. As is expected, for $\epsilon_* < 1$ the field starts to decay slowly at $t \approx H_*^{-1}$, for $\epsilon_* \geq 1$ it starts to falls down toward the slow-roll plateau at $t = \epsilon_*^{-1/2}H_*^{-1}$ and its energy density decays in proportion to $1/a_R^2$, i.e. tracking.

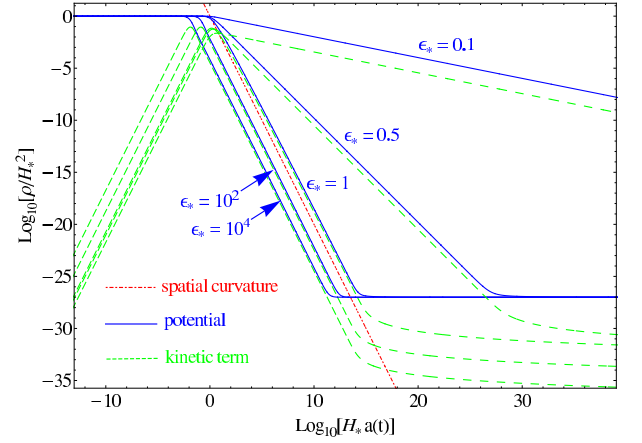


FIG. 4: The evolution of the energy densities in the region R with the exponential-type potential defined by Eq. (18) with $\epsilon_* = 0.1, 0.5, 1, 10^2$ and 10^4 . The dotted line in red is the contribution from the spatial curvature, the solid curves in blue are the potential energy and the dot-dashed curves in green are the kinetic energy.

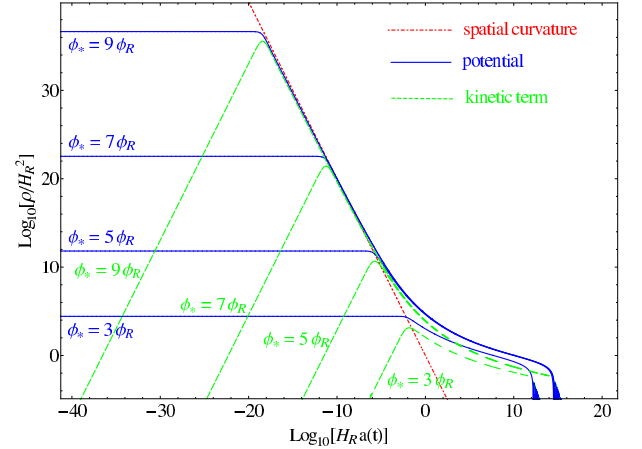


FIG. 5: The same as Fig. 4, but when the potential of the field is given by Eq. (19) with $\phi_* = 9\phi_R, 7\phi_R, 5\phi_R$, and $3\phi_R$.

The second model is a variant of the potential for the chaotic inflation:

$$\frac{\kappa}{3}V(\phi) = H_R^2 \left(\frac{\phi}{\phi_R}\right)^2 \exp\left[\frac{\phi^2 - \phi_R^2}{\phi_R^2}\right]. \quad (19)$$

The slow-roll parameter is given by

$$\epsilon(\phi) = \frac{2}{\kappa\phi_R^2} \left(\frac{\phi}{\phi_R} + \frac{\phi_R}{\phi}\right)^2. \quad (20)$$

Note that we will impose $\kappa\phi_R^2 > 8$ for the slow-roll inflation to occur at $\phi = \phi_R$. As with the exponential-type potential, the potential of a similar-type also often appears in supergravity and superstring theory. As a concrete example, we will consider the case with $H_R^2 =$

$10^{-40} M_{\text{pl}}^2$ and $\phi_R = 7.5 M_{\text{pl}}$. In Fig. 5, the evolution of the energy densities for $\phi_* = 9\phi_R, 7\phi_R, 5\phi_R$, and $3\phi_R$ is shown. Since the field varies slowly near the nucleation point, the chaotic-type potential Eq. (19) can be approximated there by the exponential-type. Therefore one can see that the tracking solution appears after $t \approx \epsilon_*^{-1/2} H_*^{-1}$ even in this chaotic-type potential.

III. CMB ANISOTROPY IN THE LANDSCAPE

A. Tensor power spectrum

We begin with reviewing how to compute the CMB power spectrum due to tensor perturbation for single-field models of one-bubble open inflation, following Refs. [32, 33]. Assuming that the observer is at the center of the spherical coordinates, the relevant tensor perturbation is the even parity one. We introduce the variable U_p to expand the spatial metric perturbation

$$\delta g_{ij} = a_C^2(\eta_C) \sum \hat{a}_{p\ell m}^{(\text{T})} U_p(\eta_C) Y_{ij}^{(+)\ell m}(\chi_C, \Omega) + \text{h.c.} \quad (21)$$

where $\hat{a}_{p\ell m}^{(\text{T})}$ and $Y_{ij}^{(+)\ell m}$ denote the annihilation operator and the analytic continuation of the even parity tensor harmonics on the 3-hyperboloid [43], respectively. The function $Y_{ij}^{(+)\ell m}$ is more explicitly expressed using the ordinary spherical harmonics $Y_{\ell m}$. In Sachs-Wolfe formula we only need the $\chi\chi$ component, which is given by

$$Y_{\chi\chi}^{(+)\ell m}(\chi_C, \Omega) = \frac{1}{\cosh^2 \chi_C} f^{p\ell}(\chi_C) Y_{\ell m}(\Omega). \quad (22)$$

Then, the time evolution equation for $f^{p\ell}(\chi_C)$ is in a model independent manner given by

$$\left[-\frac{1}{\cosh^2 \chi_C} \frac{d}{d\chi_C} \cosh^2 \chi_C \frac{d}{d\chi_C} - \frac{\ell(\ell+1)}{\cosh^2 \chi_C} \right] f^{p\ell} = (p^2 + 1) f^{p\ell}. \quad (23)$$

As a natural vacuum state after tunneling, we adopt the Euclidean vacuum, which is specified by requiring that the positive frequency functions are all regular at $\chi_C = 0$. Then, we have

$$f^{p\ell}(\chi_C) = \sqrt{\frac{\Gamma(ip + \ell + 1)\Gamma(-ip + \ell + 1)}{\Gamma(ip)\Gamma(-ip)}} \times \frac{1}{\sqrt{\cosh \chi_C}} P_{ip-1/2}^{-\ell-1/2}(i \sinh \chi_C), \quad (24)$$

where P_ν^μ is the associated Legendre function of the first kind. We have fixed the normalization constant so that the analytic continuation of $Y^{p\ell m}(\chi_C, \Omega) \equiv f^{p\ell}(\chi_C) Y_{\ell m}(\Omega)$ to region R or L behaves as a spatial harmonic function properly normalized on a unit 3-hyperboloid.

The equation for U_p is the same as the one for the massless scalar field [28]:

$$\left[\frac{1}{a_C^3} \frac{d}{d\eta_C} a_C^3 \frac{d}{d\eta_C} + \frac{p^2 + 1}{a_C^2} \right] U_p = 0. \quad (25)$$

It is also convenient to introduce another variable \mathbf{w}^p , which is related to U_p by [32, 33]

$$U_p = -\sqrt{\frac{\kappa}{p(1+p^2) \sinh \pi p}} \frac{1}{a_R} \frac{d}{dt_R} (a_R \mathbf{w}^p). \quad (26)$$

Then, the spatial eigenfunction \mathbf{w}^p satisfies a simple equation

$$\left[-\frac{d^2}{d\eta_C^2} + U_T(\eta_C) \right] \mathbf{w}^p = p^2 \mathbf{w}^p, \quad (27)$$

with

$$U_T(\eta_C) = \frac{\kappa}{2} \phi'^2(\eta_C), \quad (28)$$

where a prime represents differentiation with respect to the conformal time. Since the effective potential U_T is clearly positive definite, there is no supercurvature mode (bound state) in the tensor-type perturbation.

From the boundary conditions for the background solution, we find that the potential U_T vanishes at both boundaries of the region C. Hence, the asymptotic solutions of \mathbf{w}^p are given by plane waves. We take the two orthogonal solutions $\mathbf{w}_{C(\pm)}^p$ having the asymptotic behavior

$$i\mathbf{w}_{C(\pm)}^p \rightarrow \begin{cases} \rho_\pm^p e^{\pm ip\eta_C} + e^{\mp ip\eta_C}, & (\eta_C \rightarrow \pm\infty) \\ \sigma_\pm^p e^{\mp ip\eta_C}, & (\eta_C \rightarrow \mp\infty) \end{cases} \quad (29)$$

as independent solutions. The reflection and transmission coefficients satisfy the Wronskian relations:

$$|\rho_\pm^p|^2 + |\sigma_\pm^p|^2 = 1, \quad \sigma_+^p = \sigma_-^p, \quad \sigma_+^p \overline{\rho_-^p} + \overline{\sigma_-^p} \rho_+^p = 0. \quad (30)$$

Using the relation between the coordinates (6), we analytically continue Eq. (27) to the region R. Then, we obtain the evolution equation for \mathbf{w}^p ,

$$\left[-\frac{d^2}{d\eta_R^2} + U_T(\eta_R) - p^2 \right] \mathbf{w}^p = 0. \quad (31)$$

Similarly, the analytic continuations of the two independent modes to the region R are given by

$$\mathbf{w}_{R(+)}^p = e^{\pi p/2} \rho_+^p \overline{\tilde{\mathbf{w}}^p} + e^{-\pi p/2} \tilde{\mathbf{w}}^p, \quad (32)$$

$$\mathbf{w}_{R(-)}^p = e^{\pi p/2} \sigma_-^p \overline{\tilde{\mathbf{w}}^p}. \quad (33)$$

where $\tilde{\mathbf{w}}^p$ is the solution of Eq. (31) that asymptotically behaves like $\tilde{\mathbf{w}}^p \rightarrow e^{ip\eta_R}$ in the limit $\eta_R \rightarrow -\infty$. The amplitude of the fluctuation is proportional to the sum

of squares of these two independent modes, which is evaluated as

$$|\mathbf{w}_{R(+)}^p|^2 + |\mathbf{w}_{R(-)}^p|^2 = 2 \left[|\tilde{\mathbf{w}}^p|^2 \cosh \pi p + \text{Re} \left(\rho_+^p \left(\overline{\tilde{\mathbf{w}}^p} \right)^2 \right) \right]. \quad (34)$$

After the horizon crossing, $a^2 H^2 \gg p^2 + 1$, Eq. (25) implies that the amplitude of U_p freezes. In terms of \mathbf{w}^p , two independent solutions after the horizon crossing are given by

$$\mathbf{w}_1^p \propto a_R^{-1}, \quad \mathbf{w}_2^p \propto a_R^{-1} \int^\eta a_R^2(\eta') d\eta'. \quad (35)$$

Neglecting the decaying mode \mathbf{w}_1^p , we denote the asymptotic behavior of $\tilde{\mathbf{w}}^p$ as

$$\tilde{\mathbf{w}}^p \rightarrow -\mathbb{H}_p e^{ip\eta_T^p} a_R^{-1} \int^\eta a_R^2(\eta') d\eta', \quad (36)$$

where \mathbb{H}_p and η_T^p are the amplitude and phase, respectively. We note that $p\eta_T^p$ vanishes in the limit $p \rightarrow 0$ because $\overline{\tilde{\mathbf{w}}^p} = \tilde{\mathbf{w}}^{-p}$.

Using \mathbb{H}_p and η_T^p , the even parity tensor power spectrum can be expressed as [32, 33]

$$\begin{aligned} \frac{p^3}{2\pi^2} P_T(p) &\equiv \frac{p^3}{2\pi^2} \left(|U_{p(+)}|^2 + |U_{p(-)}|^2 \right) \\ &= 4\kappa \left(\frac{\mathbb{H}_p}{2\pi} \right)^2 \frac{p^2 \coth \pi p}{1 + p^2} (1 - y_T^p), \end{aligned} \quad (37)$$

where

$$y_T^p = -\frac{1}{\cosh \pi p} \text{Re} \left(\rho_+^p e^{-2ip\eta_T^p} \right), \quad (38)$$

essentially represents the effects of the bubble wall.

To summarize, in order to find the power spectrum for tensor-type perturbations, one has to solve the scattering problem (27) in the region C to obtain ρ_+^p and the evolution equation (36) in the region R to obtain \mathbb{H}_p and η_T^p .

Our main focus in this paper is on the latter process. Investigating the various possibilities for the tunneling potential is beyond the scope of this paper. We simply use the known results under thin-wall approximation [29]. For a thin-wall bubble, the effective potential U_T is characterized by two constant parameters, η_W and Δs :

$$U_T(\eta_C) \approx \Delta s \delta(\eta_C - \eta_W), \quad (39)$$

It can be shown that η_W and Δs are expressed in terms of the vacuum energies and the surface tension of the wall, $S_1 = \int dt_C \dot{\phi}^2$, as

$$\Delta s = \frac{2}{\sqrt{(\alpha + 1)^2 + 4\beta}}, \quad (40)$$

$$\eta_W = \frac{1}{2} \ln \left(\frac{[\sqrt{(\alpha + 1)^2 + 4\beta} + \alpha + 1]^2}{4\beta} \right), \quad (41)$$

with

$$\alpha = \frac{4(H_L^2 - H_*^2)}{\kappa^2 S_1^2}, \quad \beta = \left(\frac{2H_*}{\kappa S_1} \right)^2, \quad (42)$$

where $H_L = \sqrt{\kappa V(\phi_L)/3}$ and $H_* = \sqrt{\kappa V(\phi_*)/3}$.

In terms of η_W and Δs , we can solve the equation for the mode function (27) to obtain the reflection coefficient ρ_+ :

$$\rho_+^p = \frac{-ie^{2ip\eta_W} \Delta s}{2p + i\Delta s}. \quad (43)$$

From Eq. (30), the transmission probability from the false vacuum is given by $|\sigma_+^p|^2 = 1/[1 + (\Delta s/2p)^2]$. From this expression, we find that efficiently reflected at the wall are only low frequency modes with $p \lesssim \Delta s/2$, which are thought to be interpreted as the wall fluctuation [29]. Notice that the reflection rate at $p = 0$ is unity. Without this reflection by the wall, the square amplitude of fluctuation is divergent. In this sense, one might be able to interpret that the so-called wall fluctuation mode represents the penetration of the waves from the false vacuum side, and its amplitude is reduced if the wall efficiently reflects back the waves. Substituting the expression (43), the spectrum becomes

$$\begin{aligned} \frac{p^3}{2\pi^2} P_T(p) &= 4\kappa \left(\frac{\mathbb{H}_p}{2\pi} \right)^2 \frac{p^2 \coth \pi p}{1 + p^2} \\ &\times \left[1 - \frac{(\Delta s)^2 \cos[b_p p] + 2p\Delta s \sin[b_p p]}{[4p^2 + (\Delta s)^2] \cosh \pi p} \right], \end{aligned} \quad (44)$$

where $b_p := 2(\eta_W - \eta_T^p)$. Once parameters $\eta_W, \Delta s$ and the late-time asymptotic value of $\tilde{\mathbf{w}}^p$ are fixed, we can immediately calculate the power spectrum using this formula. The power spectra for the tensor-type perturbation are shown in Fig. 6 for $(\alpha, \beta) = (100, 1), (1, 100), (10^{-3}, 10^{-3})$ and $(1, 1)$, setting $\mathbb{H}_p = H_R$ and $\eta_T^p = 0$. As a reference, we plot the spectrum for $\mathbb{H}_p = H_R, \Delta s = \infty$ and $b_p = 0$, which we denote by ‘‘plain spectrum’’ in this paper, as a dashed curve in black in the same figure.

B. Effects of inflation in the open universe

Now we move on to the problem to solve the evolution equation (36) in the region R to evaluate \mathbb{H}_p and η_T^p .

1. Slow-roll case

We begin by the case with $\epsilon_* \ll 1$. From the discussion in Sec. II B, there is no rapid roll phase for $\epsilon_* \ll 1$, and the field kinetic term is always irrelevant for the cosmic expansion rate. In this case one can neglect the potential U_T in the field equation for the mode function \mathbf{w}^p (31). Hence, \mathbf{w}^p behaves like a plane wave and its

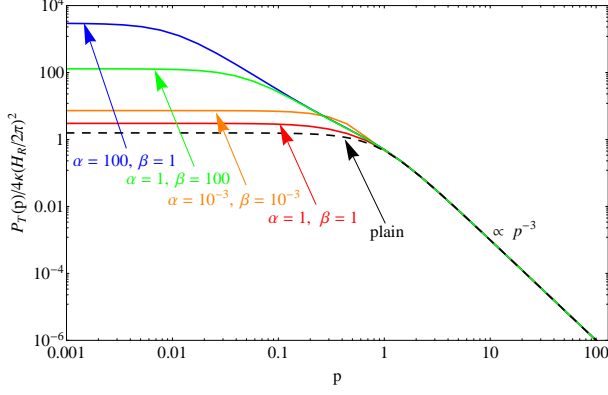


FIG. 6: The power spectrum due to tensor-type perturbation. The solid curves are, from top to bottom, for $(\alpha, \beta) = (100, 1)$, $(1, 100)$, $(10^{-3}, 10^{-3})$ and $(1, 1)$, setting $\mathbb{H}_p = H_R$ and $\eta_T^p = 0$. The dashed curve in black is the spectrum for $\Delta s = \infty$ and $b_p = 0$, which we call “plain spectrum”.

amplitude stays constant. The scale factor will also be approximated by $a_R \approx -1/H_R \eta$ in this case. Then, from Eq. (36), we find $\mathbb{H}_p \approx H_R$ and $\eta_T^p \approx 0$. Namely, the plain spectrum is obtained. As seen from the formula (44), the amplitude of tensor perturbation is basically scale invariant ($P_T \propto p^{-3}$) whose amplitude is determined by the Hubble rate inside the bubble, except for the modes near $p = 0$. For the modes with $p \lesssim \Delta s$, there is suppression due to the reflection by the wall as mentioned earlier, and hence the spectrum P_T does not grow indefinitely for small p . In Fig. 6, we plot the power spectrum due to tensor-type perturbation with $\mathbb{H}_p = H_R$, $\eta_T^p = 0$ and various tunneling parameters α, β .

This result tells us that there is no memory from the high energy false vacuum in large p modes. In other words, the high frequency modes simply stay in the adiabatic vacuum state irrespective of the presence of the bubble wall and the initial high energy vacuum.

This can be also understood as follows. It will be natural to assume that the partial wave U_p typically has the amplitude of $O(H_*/M_{\text{pl}})$ as a memory of the high energy false vacuum when the physical wavelength is as short as H_*^{-1} . At this initial time the scale factor will be given by $a_{\text{R,init}} = \sqrt{p^2 + 1}/H_*$. On the other hand, the freeze-out of the amplitude of U_p occurs at around the horizon crossing time, at which the scale factor is estimated as $a_{\text{R,final}} = \sqrt{p^2 + 1}/H_R$. As the scale factor evolves from $a_{\text{R,init}}$ to $a_{\text{R,final}}$, the amplitude of the tensor-type perturbation U_p before the horizon crossing decays in proportion to $1/a_R$. Hence, the amplitude frozen after the horizon crossing would be estimated as

$$p^{3/2}|U_p| \approx \frac{H_*}{M_{\text{pl}}} \frac{a_{\text{R,init}}}{a_{\text{R,final}}} \approx \frac{H_R}{M_{\text{pl}}}. \quad (45)$$

The amplitude of the spectrum is solely determined by H_R independently of the initial value of the Hubble pa-

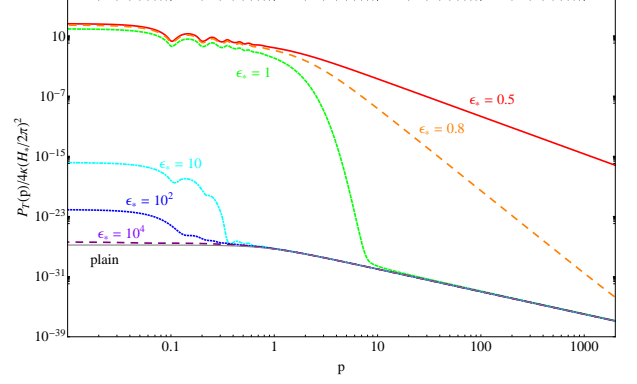


FIG. 7: The tensor-type power spectrum with the exponential-type potential Eq. (18). The solid curves are, from top to bottom, the spectrum with $\epsilon_* = 0.5, 0.8, 1, 10, 10^2$ and 10^4 . Here we set $\alpha = 1$ and $\beta = 1$ as typical parameters for which the contribution from the wall fluctuation mode is negligible small. For comparison, we also plot the plain spectrum in the gray.

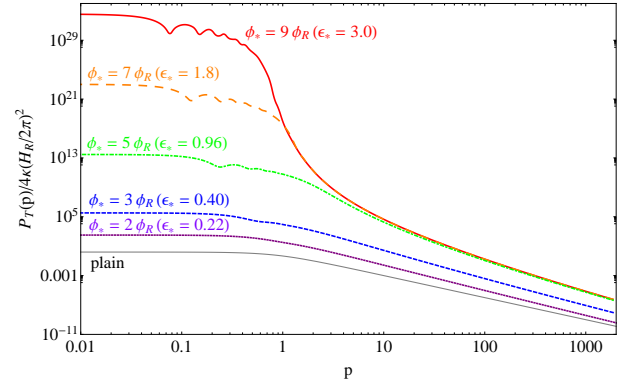


FIG. 8: The same as Fig. 7, but the potential of the field is given by Eq. (19) with $\phi_* = 9\phi_R, 7\phi_R, 5\phi_R, 3\phi_R$, and $2\phi_R$.

rameter H_* . This rough estimate explains the model-independent behavior of the tensor perturbation spectrum in the high frequency region.

2. Rapid roll case

Next we consider the models with the long-lasting rapid roll phase in the region R. In Fig. 7, we present the computed tensor perturbation spectra for the exponential-type model defined by Eq. (18), setting $\alpha = 1$ and $\beta = 1$ as typical parameters for which the contribution from the wall fluctuation mode is negligible small. As seen from the figure, the spectra are quite different from the plain spectrum, for which we neglect not only the contribution of the wall fluctuation mode but also the effect of the field dynamics in the region R. The

power spectrum for $\epsilon_* = \mathcal{O}(1)$ increases sharply for small p , i.e. highly red-tilted. As we discussed in Sec. II B, in this case the curvature length is well outside the horizon size during the tracking phase. Since the amplitude for small p depends on the value of the Hubble rate at the time when the curvature scale starts to deviate from the horizon size, it keeps the memory of the high expansion rate of $\mathcal{O}(H_*)$ at the onset of the rapid roll phase. Therefore the squared amplitude for small p is proportional to $\mathcal{O}(\kappa H_*^2)$. In contrast, the wavelength of the modes with sufficiently large p stays inside the horizon size during the tracking phase. Only after the field arrives at the slow-roll plateau, these modes cross the horizon. Thus, the squared amplitude of the modes with large p becomes $\mathcal{O}(\kappa H_R^2)$. For this reason, the spectrum for $\epsilon_* = \mathcal{O}(1)$ is steeply red-tilted.

By contrast, if the potential is extremely steep, $\epsilon_* \gg 1$, at the nucleation point, the field starts to roll down rapidly before the curvature term becomes irrelevant for the expansion of the universe. As long as the potential continues to be steep enough, the curvature length stays comparable to the horizon size. If this remains to be the case until the field reaches the slow-roll plateau, even the amplitude of the modes with $p \lesssim 1$ is governed by the Hubble rate at the slow-roll plateau, H_R . Therefore there is no significant enhancement of the amplitude for small p in this case.

Finally, the spectrum for $\epsilon_* \ll 1$ can be understood in the usual manner. The spectrum is similar to the one presented in Fig. 6, in which the field dynamics in the region R is neglected. The same plot for the chaotic-type model defined by Eq. (19) is shown in Fig. 8. As with the exponential-type model, the spectra for $\epsilon_* = \mathcal{O}(1)$ have large enhancement for small p , while the spectra with $\epsilon_* < 1$ are similar to the one presented in Fig. 6. As the initial position ϕ_* is increased, the magnitude for large p decreases because it is normalized by the Hubble parameter at the nucleation point H_* , which becomes larger.

C. CMB temperature anisotropy

We translate the spectrum for tensor-type perturbation obtained in the preceding subsection into CMB temperature anisotropies, following the discussion given in Ref. [29]. The large-angle CMB temperature anisotropies due to tensor-type perturbation are simply evaluated by the Sachs-Wolfe formula

$$\frac{\Delta T}{T}(\hat{n}) = -\frac{1}{2} \int_{\eta_{\text{LSS}}}^{\eta_0} d\eta g'_{ij}(\eta, x^i(\eta)) \hat{n}^i \hat{n}^j, \quad (46)$$

where η_0 and η_{LSS} , respectively, denote the conformal time at the present epoch and that at the last scattering surface, \hat{n}^i is the unit vector along the observer's line-of-sight and $x^i(\eta) = (\eta_0 - \eta) \hat{n}^i$ represents the photon trajectory.

Since we are interested in the anisotropies on large angular scales, we consider only those modes that enter the Hubble horizon after the universe becomes matter dominated. Thus, we set the scale factor to $a(\eta) = \cosh \eta - 1$. The conformal time then can be written in terms of the density parameter Ω_0 and the redshift z :

$$\eta(z) = 2 \text{arccosh} \sqrt{1 + \frac{\Omega_0^{-1} - 1}{1 + z}}, \quad (47)$$

where we have neglected the effect of the dark energy.

The evolution equation for U is given by [44]

$$U_p'' + 2 \frac{a'}{a} U_p' + (p^2 + 1) U_p = 0. \quad (48)$$

The above equation can be solved exactly to give

$$U_p(\eta) = U_p(0) G_p(\eta), \quad (49)$$

where $U_p(0)$ is the initial amplitude of fluctuations given by Eq. (37) and

$$G_p(\eta) = \frac{3 \left(\cosh\left(\frac{\eta}{2}\right) \frac{\sin p\eta}{2p} - \sinh\left(\frac{\eta}{2}\right) \cos p\eta \right)}{(1 + 4p^2) \sinh^3\left(\frac{\eta}{2}\right)}, \quad (50)$$

is the growing mode function. Now, we decompose the temperature anisotropies in terms of the spherical harmonics:

$$\frac{\Delta T}{T}(\hat{n}) = \sum_{\ell, m} \int_0^\infty dp \left(\frac{\Delta T}{T} \right)_{p, \ell} Y_{\ell m}(\hat{n}), \quad (51)$$

where

$$\begin{aligned} \left(\frac{\Delta T}{T} \right)_{p, \ell} Y_{\ell m} &= -\frac{1}{2} U_p(0) \\ &\times \int_{\eta_{\text{LSS}}}^{\eta_0} d\eta G_p'(\eta) Y_{\chi\chi}^{p\ell m}(\eta_0 - \eta, \Omega), \end{aligned} \quad (52)$$

and the radial-radial component of the tensor-type harmonic function $Y_{\chi\chi}^{p\ell m}(\chi, \Omega)$ is given by

$$\begin{aligned} Y_{\chi\chi}^{p\ell m}(\chi, \Omega) &= \sqrt{\frac{1}{2(p^2 + 1)} \frac{(\ell + 2)!}{(\ell - 2)!}} \\ &\times \left| \frac{\Gamma(\ell + 1 + ip)}{\Gamma(1 + ip)} \right| \frac{P_{ip-1/2}^{-\ell-1/2}(\cosh \chi)}{\sinh^{5/2} \chi} Y_{\ell m}(\Omega). \end{aligned} \quad (53)$$

The temperature anisotropies are usually expressed in terms of C_ℓ , the multipole moments of the temperature autocorrelation function, defined by

$$\left\langle \frac{\Delta T}{T}(\hat{n}) \frac{\Delta T}{T}(\hat{n}') \right\rangle = \frac{1}{4\pi} \sum_\ell (2\ell + 1) C_\ell P_\ell(\cos \theta), \quad (54)$$

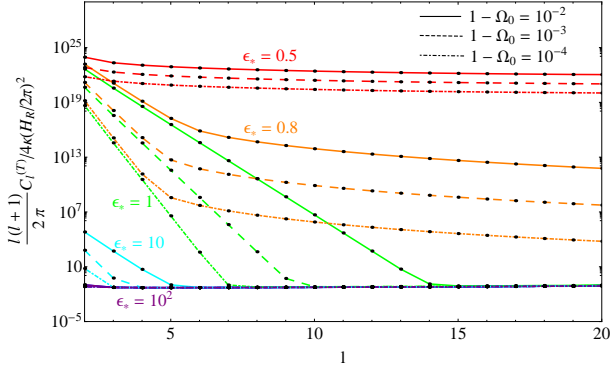


FIG. 9: The multipole moments for the tensor type perturbations for the exponential-type potential Eq. (18) with $\epsilon_* = 0.5, 0.8, 1, 10$ and 10^2 . Again we set $\alpha = 1$ and $\beta = 1$ as a representative case.

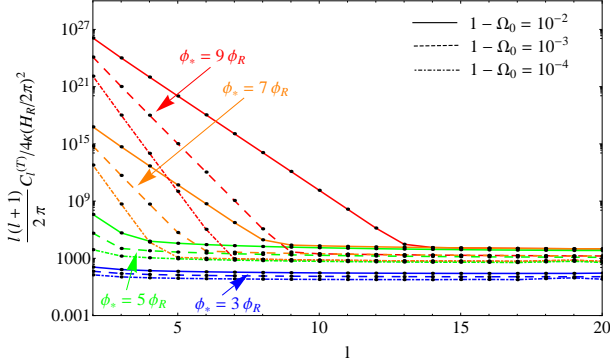


FIG. 10: The same as Fig. 9, but when the field potential is given by Eq. (19) with $\phi_* = 9\phi_R, 7\phi_R, 5\phi_R$, and $3\phi_R$.

where $\cos\theta = \hat{\mathbf{n}} \cdot \hat{\mathbf{n}}'$. Then, the multipole moments for the tensor-type perturbation $C_\ell^{(T)}$ are given by

$$C_\ell^{(T)} = \int_0^\infty dp \left\langle \left| \frac{\Delta T}{T} \right|_{p,\ell}^2 \right\rangle = \frac{1}{8} \frac{(\ell+2)!}{(\ell-2)!} \int_0^\infty dp \frac{P_T(p)}{p^2+1} \left| \frac{\Gamma(\ell+1+ip)}{\Gamma(1+ip)} \right|^2 \times \left| \int_{\eta_{LSS}}^{\eta_0} d\eta G'_p(\eta) \frac{P_{ip-1/2}^{-\ell-1/2}(\cosh(\eta_0-\eta))}{\sinh^{5/2}(\eta_0-\eta)} \right|^2. \quad (55)$$

We will discuss possible observational signatures in the CMB temperature anisotropies in the open inflation scenario revived in the context of string theory landscape that prefers a moderately small value of $1 - \Omega_0$. The value of Ω_0 depends rather sensitively on the underlying scenario. The prediction for the value of Ω_0 , based on the primordial distribution of the number of the e-folds of the inflation inside the bubble and the anthropic bias, was investigated in [17, 19]. There is a big uncertainty because the resulting distribution of the value of Ω_0 strongly de-

pends on the choice of the probability measure, but their estimates implies that it can be natural that $1 - \Omega_0$ is in the marginally observable range. For this reason, we focus on the case that $1 - \Omega_0$ is in the observable range, e.g. from 10^{-3} to 10^{-2} , and evaluate the CMB anisotropies for the previously introduced two toy models.

The computed CMB temperature power spectra for the exponential-type and chaotic-type models are shown in Figs. 9 and 10, respectively. Again we set $\alpha = 1$ and $\beta = 1$ as a representative case in which the contribution from the wall fluctuation mode is negligible small. One can see that the tensor CMB angular power spectrum for small ℓ behaves like $(1 - \Omega_0)^\ell$, while it agrees with the scale invariant inflationary tensor spectrum for large ℓ . Compared with the amplitude of the tensor perturbation for the slow-roll inflation at $H \approx H_R$, there is significant enhancement for small ℓ due to the field dynamics in the region R for $\epsilon_* \lesssim 1$. Hence, we find that, unless ϵ is not extremely large, rapid rolling down affects the CMB spectrum at low ℓ significantly.

It is known that the spectrum Eq. (55) can be approximately decomposed into two pieces:

$$C_\ell^{(T)} = P_W \tilde{C}_\ell^{(W)} + C_\ell^{(T, \text{res})}, \quad (56)$$

where $P_W \tilde{C}_\ell^{(W)}$ represent contributions due to wall fluctuations:

$$P_W = \int_0^\infty dp P_T(p), \quad (57)$$

$$\tilde{C}_\ell^{(W)} = \frac{(\ell+2)!(\ell!)^2}{8(\ell-2)!} \times \left| \int_{\eta_{LSS}}^{\eta_0} d\eta G'_0(\eta) \frac{P_{-1/2}^{-\ell-1/2}(\cosh(\eta_0-\eta))}{\sinh^{5/2}(\eta_0-\eta)} \right|^2. \quad (58)$$

We have also introduced $C_\ell^{(T, \text{res})}$, which corresponds to the continuous spectrum due to standard tensor perturbations, as the residual piece of the spectrum. The previous plots presented in Figs. 9 and 10 are basically corresponding to $C_\ell^{(T, \text{res})}$.

The effect of the wall fluctuation mode is rather easy to investigate analytically, and in many cases it is more important than the continuum modes. To see observational signatures when the deviation of Ω_0 from unity is small, it will be useful to expand quantities with respect to $1 - \Omega_0$. The spectrum due to the wall fluctuations given by Eq. (58) reduces to

$$\frac{\ell(\ell+1)}{2\pi} \tilde{C}_\ell^{(W)} \approx \frac{(\ell+2)!(\ell+1)!}{800\pi(\ell-1)\Gamma(\ell+3/2)} (1 - \Omega_0)^\ell. \quad (59)$$

Unless $1 - \Omega_0$ is close to unity, the effects of wall fluctuation mode mainly appear in the quadrupole of CMB temperature fluctuation.

The amplitude of the wall fluctuation mode can be also evaluated analytically. As seen in Figs. 6, 7, and 8,

the integral (58) is dominated by the contribution from p around 0. Thus, we expand $P_T(p)$ around $p = 0$ as

$$\begin{aligned} \frac{1}{2\pi^2} P_T(p) &\approx \frac{4\kappa}{\pi} \left(\frac{\mathbb{H}_0}{2\pi} \right)^2 \frac{1}{p^2 + (\Delta s/2)^2} \\ &\times \left[1 - \left(\frac{b_0 \Delta s}{2} \right) \frac{\sin[b_0 p]}{b_0 p} + \frac{1}{2} \left(\frac{b_0 \Delta s}{2} \right)^2 \frac{\sin^2 \left[\frac{b_0 p}{2} \right]}{\left[\frac{b_0 p}{2} \right]^2} \right], \end{aligned} \quad (60)$$

where we assumed that $p \ll 1$ but the combination $b_0 p$ is not necessarily small. Notice that $b_p = 2(\eta_W - \eta_T^p)$ also depends on the field dynamics in the region R through η_T^p , which can be large. Substituting Eq. (60) into Eq. (57), we find that the amplitude due to wall fluctuations can be approximated by

$$\frac{P_W}{2\kappa H_*^2} \approx \frac{1}{\Delta s} \left(\frac{\mathbb{H}_0}{H_*} \right)^2 f \left(\frac{\Delta s b_0}{2} \right), \quad (61)$$

with

$$f(x) = 2e^{-(x+|x|)/2} - 1 + x. \quad (62)$$

This expression (61) is valid even if $\Delta s |b_0|$ is large. The expression contains exponential but, in fact, $f(x)$ is just $x - 1$ for $x \gg 1$, while $f(x) \approx x + 1$ for $x \lesssim 1$. Therefore, P_W only weakly depends on η_T^0 . Roughly speaking, the above expression indicates that the amplitude of the wall fluctuations can be significantly enhanced only when $(\mathbb{H}_0/H_*)^2/\Delta s$ is large. Small Δs can be realized for a small wall tension S_1 since Δs is roughly estimated as $\Delta s \approx \kappa S_1/2H_*$ when H_L and H_* are the same order. An interesting observation is that the amplitude of wall fluctuation also depends on \mathbb{H}_0 . Therefore, when the continuum contribution $C_\ell^{(T, \text{res})}$ for small ℓ is enhanced due to the evolution inside the region R, the wall fluctuation mode is also enhanced.

It is shown in Fig. 11 how the amplitude of $C_2^{(T)}$ depends on ϵ for the case of the exponential-type model defined by Eq. (18). The value of $1 - \Omega_0$ is fixed to 10^{-3} here. In these plots the magnitude is rescaled by multiplying Δs . This figure shows that the power for the quadrupole increases for small Δs precisely in proportion to $1/\Delta s$ for $\epsilon_* \gtrsim 1$ as expected. For $\epsilon_* \lesssim 1$, the contribution from continuum becomes significantly large. As a result, the magnitude becomes larger for a smaller value of Δs .

It may be noted that both modes at $p \approx 0$ and at $p \gtrsim 1$ contribute to the CMB quadrupole, but the former modes physically represent the wall fluctuation degree of freedom. Therefore they might have a property similar to the scalar-type perturbation. Thus these two different contributions might be distinguished by looking at the CMB polarization.

If a model predicts large enhancement of low ℓ modes due to tensor perturbation, such a model may contradict the current observation. This gives a constraint on the model building based on string theory. We are interested

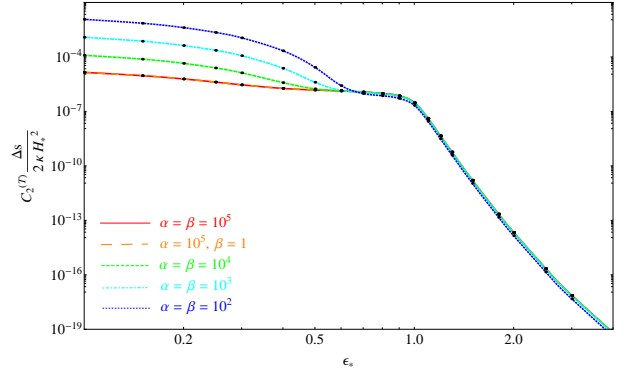


FIG. 11: CMB quadrupole amplitude as a function of ϵ_* for various values of (α, β) : $(10^2, 10^2)$, $(10^3, 10^3)$, $(10^4, 10^4)$, $(10^5, 10^5)$ and $(10^5, 1)$. They corresponds to $\Delta s \approx 2 \times 10^{-2}$, 2×10^{-3} , 2×10^{-4} , 2×10^{-5} and 2×10^{-5} , respectively. The value of $1 - \Omega_0$ is fixed to 10^{-3} . Here the amplitude multiplied by Δs is shown. Therefore these plots clearly show that the quadrupole amplitude scales like $1/\Delta s$ for $\epsilon_* \gtrsim 1$.

in the case when H_* is close to Planck scale but inflation in the region R occurs at sufficiently low energies. We also require $1 - \Omega_0$ is not extremely small. As advocated by Freivogel et al. [17], this may be achieved naturally in the string landscape.

Then, first of all, a very small ϵ_* is not compatible with the above scenario because the slow-roll inflation phase starts before the energy density decays sufficiently. This means that the amplitude of the tensor perturbation is too large. When $\epsilon_* \gg 1$, the contribution to the CMB spectrum from the tensor perturbation is largely suppressed by the factor $(\mathbb{H}_0/H_*)^2$. Even if $\epsilon_* = O(1)$, there is a suppression factor $(1 - \Omega_0)^\ell$. On the other hand, there is a possible huge enhancement factor $\sim 1/\Delta s$ due to the wall fluctuation mode, which can be very large if the wall tension is small. However, one cannot choose a very small Δs in the present context when H_* is close to the Planck scale. An extremely small Δs is in conflict with the requirement that the bubble nucleation rate is sufficiently suppressed in order to avoid too large a signature of bubble collisions in our observable universe.

The above three factors, the values of ϵ_* , Δs and $1 - \Omega_0$ basically control the amplitude of the CMB spectrum for small ℓ due to the tensor perturbation, which is observationally constrained to be not too large. We should stress that the constraint from the tensor contribution can be avoided if one can arrange the potential slope after the bubble nucleation to be sufficiently steep, i.e., if $\epsilon_* \gg 1$.

In this paper, we did not study how the factor coming from the tunneling process, which is $1/\Delta s$ in the thin wall case, is related to the tunneling potential beyond the thin wall approximation. For example, we did not discuss the case that the energy density at the nucleation point is already largely reduced, in spite of the high false vacuum energy. Such a tunneling process cannot be described by

the thin wall approximation. We will come back to this issue in our future publication.

IV. SUMMARY

The inflation scenario with Coleman-De Luccia (CDL) tunneling, the so-called open inflation has attracted renewed attention in the context of string landscape. The most important cosmological consequence in the string landscape is that it is likely that there were a sequence of tunneling events in our past and our universe is produced inside a bubble.

In this paper we focused on those models that experience the CDL tunneling followed by the last inflation before the beginning of our hot Friedmann universe inside a nucleated bubble. Our interest was in the landscape scenario in which the energy density at the nucleation point is close to the Planck scale, while a much lower energy scale is preferred for this last inflation inside the nucleated bubble. We also assumed a moderately small $1 - \Omega_0$ preferred from a perspective of the anthropic probability distribution. Under these assumptions we examined the CMB temperature anisotropies due to the tensor-type perturbation.

We considered single-field models, assuming that the condition for the presence of a CDL instanton $V'' > \kappa V$ is satisfied around the potential barrier. In this case it seems difficult to imagine that such a potential is connected to the one that satisfies one of the slow-roll conditions $V'' < \kappa V$ immediately after tunneling. Therefore it seems fairly natural to have some intermediate stage of rapid rolling down after tunneling. We found that a rapid-roll phase significantly modifies the power spectrum of the tensor-type perturbations. In particular, the behavior of the power spectrum strongly depends on the slow-roll parameter at the nucleation point, ϵ_* , where $\epsilon \equiv (V'/V)^2/(2\kappa)$ as defined in Eq. (12).

When $\epsilon_* \lesssim 1$, there is no rapid-roll phase. Then, the high rate of cosmic expansion near the nucleation point is imprinted in the low ℓ components of CMB and the spectrum becomes red-tilted. Such a feature would contradict the observed CMB spectrum if the the potential energy at the nucleation point were sufficiently high and $1 - \Omega_0$ were not extremely small.

As we noted in Introduction, if the transition were driven by the Hawking-Moss instanton, which is the case in the inflationary models with the simplest polynomial potential $m^2\phi^2/2 - \delta\phi^3/3 + \lambda\phi^4/4$, the large angle CMB fluctuations would be significantly enhanced due to the scalar-type perturbations. Such models would contradict current observations, unless the last stage of inflation after the tunneling is very long. A similar conclusion is valid for the quasi-open scenario, which involves more than one scalar field [20]. This scenario seems much easier, if not easiest, to implement in string theory, as compared to other options.

Thus one of the important conclusions is that we are

already testing string theory landscape against observations, and we already know quite a lot about the structure of the potential, assuming that inflation after tunneling is rather short. Note that this assumption [17] is based on a specific choice of the probability measure in eternal inflation, and on some additional assumptions about the inflationary potentials in the landscape. Our analysis shows that we can either rule out a large class of inflationary potentials which at the first glance seem quite reasonable, or we can rule out the assumption that a long stage of the slow roll inflation is improbable.

By contrast, when $\epsilon_* \gg 1$, we have a rapid-roll phase after the bubble nucleation. In this case, the CMB spectrum behaves as if there is no memory of the high energy regime. Namely, the magnitude of CMB spectrum is basically determined by the slow-roll inflation at low energies, which succeeds the rapid-roll phase. Therefore the tensor perturbations tend to be negligible, which is consistent with observations. We also note that the scalar-type perturbations are expected to be more sensitive to the evolution of the field. Since the power spectrum for gauge-invariant spatial curvature perturbation will be roughly given by $(H_R^2/\dot{\phi})^2$, one can expect that the amplitude of the scalar perturbations will be suppressed during the rapid-roll phase. Since this effect occurs at the first stages of inflation after the tunneling, it may lead to suppression of the large scale adiabatic perturbations [26, 27]. This tendency seems to fit well with the observed suppression of the CMB quadrupole moment [45].

The above conclusion is slightly modified by the presence of the wall fluctuation modes. When the wall tension S_1 is much smaller than $M_{\text{pl}}\sqrt{\rho_*}$, where ρ_* is the energy density at around the tunneling, the wall fluctuation modes enhance the low ℓ components in the CMB spectrum in proportion to $S_1^{-1}(1 - \Omega_0)^\ell$. Therefore a possible observational signature of the wall fluctuation modes is basically in the CMB quadrupole. The amplitude due to the wall fluctuation modes is also influenced by the value of ϵ_* in the same manner as that due to the continuous modes. In particular, the contribution of the wall fluctuation modes is negligible for $\epsilon_* \gg 1$ as shown in Fig. 11.

To summarize, in the context of string theory landscape, the current observational data already constrain the shape of the potential such that the slow-roll parameter $\epsilon = (V'/V)^2/(2\kappa)$ right after tunneling should be large, $\epsilon_* \gg 1$ unless $1 - \Omega_0$ is extremely small. A large value of ϵ_* also reduces the contribution of the wall fluctuation modes to the CMB spectrum, hence seems to be even preferred from the observed suppression of the CMB quadrupole.

In this paper, we focused on tensor-type perturbations. We found that the effect of the evolution of the inflaton inside a nucleated bubble affects the tensor-type power spectrum significantly. We also discussed expected signatures in the scalar-type perturbations based on previous work in the literature. Using these expected features in the CMB spectra, we can say that we are already testing

models of inflation in the context of string theory landscape. To make more definite predictions and test the landscape, detailed studies on the scalar-type perturbations are necessary. We plan to come back to this issue in the near future.

Acknowledgments

D.Y. would like to thank K. Kamada, S. Mukohyama, T. Nakamura, Y. Nambu, Y. Sendouda, L. Susskind and J. Yokoyama for valuable comments and useful sugges-

tions. This work is supported in part by Monbukagakusho Grant-in-Aid for the global COE program, “The Next Generation of Physics, Spun from Universality and Emergence” at Kyoto University. The work of M.S. was supported by JSPS Grant-in-Aid for Scientific Research (B) No. 17340075, (A) No. 18204024 and by Grant-in-Aid for Creative Scientific Research No. 19GS0219. T.T. is supported by Monbukagakusho Grant-in-Aid for Scientific Research Nos. 21111006 and 22111507. D.Y. and A.N. was supported by Grant-in-Aid for JSPS Fellow No. 20-1117 and No. 21-1899, A.L. was supported in part by NSF grant PHY-0756174 and by the FQXi grant RFP2-08-19.

-
- [1] E. Komatsu *et al.*, “Seven-Year Wilkinson Microwave Anisotropy Probe (WMAP) Observations: Cosmological Interpretation,” arXiv:1001.4538 [astro-ph.CO].
 - [2] A. D. Linde, *Particle Physics and Inflationary Cosmology* (Harwood, Chur, Switzerland, 1990) [arXiv:hep-th/0503203].
 - [3] S. Kachru, R. Kallosh, A. Linde and S. P. Trivedi, “De Sitter vacua in string theory,” Phys. Rev. D **68**, 046005 (2003) [arXiv:hep-th/0301240].
 - [4] L. Susskind, “The anthropic landscape of string theory,” arXiv:hep-th/0302219.
 - [5] B. Freivogel and L. Susskind, “A framework for the landscape,” Phys. Rev. D **70**, 126007 (2004) [arXiv:hep-th/0408133].
 - [6] S. R. Coleman, “The Fate Of The False Vacuum. 1. Semiclassical Theory,” Phys. Rev. D **15**, 2929 (1977) [Erratum-ibid. D **16**, 1248 (1977)].
 - [7] S. R. Coleman and F. De Luccia, “Gravitational Effects On And Of Vacuum Decay,” Phys. Rev. D **21**, 3305 (1980).
 - [8] J. R. Gott, “Creation Of Open Universes From De Sitter Space,” Nature **295**, 304 (1982).
 - [9] J. R. Gott and T. S. Statler, “Constraints On The Formation Of Bubble Universes,” Phys. Lett. B **136**, 157 (1984).
 - [10] M. Sasaki, T. Tanaka, K. Yamamoto and J. Yokoyama, “Quantum state inside a vacuum bubble and creation of an open universe,” Phys. Lett. B **317**, 510 (1993).
 - [11] B. Ratra, P. J. E. Peebles, “Inflation in an open universe,” Phys. Rev. D **52**, 1837-1894 (1995).
 - [12] M. Bucher, A. S. Goldhaber and N. Turok, “An open universe from inflation,” Phys. Rev. D **52**, 3314 (1995) [arXiv:hep-ph/9411206].
 - [13] M. Sasaki, T. Tanaka and K. Yamamoto, “Euclidean vacuum mode functions for a scalar field on open de Sitter space,” Phys. Rev. D **51**, 2979 (1995) [arXiv:gr-qc/9412025].
 - [14] D. H. Lyth and A. Woszczyna, Phys. Rev. D **52**, 3338 (1995) [arXiv:astro-ph/9501044].
 - [15] K. Yamamoto, M. Sasaki and T. Tanaka, “Large angle CMB anisotropy in an open universe in the one bubble inflationary scenario,” Astrophys. J. **455**, 412 (1995) [arXiv:astro-ph/9501109].
 - [16] M. Bucher and N. Turok, “Open Inflation With Arbitrary False Vacuum Mass,” Phys. Rev. D **52**, 5538 (1995) [arXiv:hep-ph/9503393].
 - [17] B. Freivogel, M. Kleban, M. Rodriguez Martinez, L. Susskind, JHEP **0603**, 039 (2006). [hep-th/0505232].
 - [18] S. Weinberg, “Anthropic Bound on the Cosmological Constant,” Phys. Rev. Lett. **59**, 2607 (1987).
 - [19] A. De Simone and M. P. Salem, “The distribution of Ω_k from the scale-factor cutoff measure,” Phys. Rev. D **81**, 083527 (2010) [arXiv:0912.3783 [hep-th]].
 - [20] A. D. Linde, “Inflation with variable Ω ,” Phys. Lett. B **351**, 99 (1995) [arXiv:hep-th/9503097]; A. D. Linde and A. Mezhlumian, “Inflation with $\Omega \neq 1$,” Phys. Rev. D **52**, 6789 (1995) [arXiv:astro-ph/9506017].
 - [21] S. W. Hawking and I. G. Moss, “Supercooled Phase Transitions In The Very Early Universe,” Phys. Lett. B **110**, 35 (1982).
 - [22] L. G. Jensen and P. J. Steinhardt, “Bubble Nucleation And The Coleman-Weinberg Model,” Nucl. Phys. B **237**, 176 (1984).
 - [23] A.A. Starobinsky, in: *Fundamental Interactions* (MGPI Press, Moscow, 1984), p. 55; A.A. Starobinsky, in: *Current Topics in Field Theory, Quantum Gravity and Strings*, Lecture Notes in Physics, eds. H.J. de Vega and N. Sanchez (Springer, Heidelberg 1986) **206**, p. 107.
 - [24] A. D. Linde, “Hard art of the universe creation (stochastic approach to tunneling and baby universe formation),” Nucl. Phys. B **372**, 421 (1992) [arXiv:hep-th/9110037].
 - [25] P. Batra and M. Kleban, “Transitions Between de Sitter Minima,” Phys. Rev. D **76**, 103510 (2007) [arXiv:hep-th/0612083].
 - [26] A. D. Linde, “A toy model for open inflation,” Phys. Rev. D **59**, 023503 (1999) [arXiv:hep-ph/9807493].
 - [27] A. D. Linde, M. Sasaki and T. Tanaka, “CMB in open inflation,” Phys. Rev. D **59**, 123522 (1999) [arXiv:astro-ph/9901135].
 - [28] T. Tanaka and M. Sasaki, “The spectrum of gravitational wave perturbations in the one-bubble open inflationary universe,” Prog. Theor. Phys. **97**, 243 (1997) [arXiv:astro-ph/9701053].
 - [29] M. Sasaki, T. Tanaka and Y. Yakushige, “Wall fluctuation modes and tensor CMB anisotropy in open inflation models,” Phys. Rev. D **56**, 616 (1997) [arXiv:astro-ph/9702174].
 - [30] M. Bucher, J. D. Cohn, “Primordial gravitational waves from open inflation,” Phys. Rev. D **55**, 7461-7479 (1997). [astro-ph/9701117].
 - [31] T. Hertog, N. Turok, “Gravity waves from instantons,” Phys. Rev. D **62**, 083514 (2000). [astro-ph/9903075].

- [32] J. Garriga, X. Montes, M. Sasaki and T. Tanaka, “Spectrum of cosmological perturbations in the one-bubble open universe,” Nucl. Phys. B **551**, 317 (1999) [arXiv:astro-ph/9811257].
- [33] J. Garriga, X. Montes, M. Sasaki and T. Tanaka, “Canonical quantization of cosmological perturbations in the one-bubble open universe,” Nucl. Phys. B **513**, 343 (1998) [arXiv:astro-ph/9706229].
- [34] K. Yamamoto, M. Sasaki and T. Tanaka, “Quantum fluctuations and CMB anisotropies in one-bubble open inflation models,” Phys. Rev. D **54**, 5031 (1996) [arXiv:astro-ph/9605103].
- [35] M. Sasaki and T. Tanaka, “Can the simplest two-field model of open inflation survive?,” Phys. Rev. D **54**, 4705 (1996) [arXiv:astro-ph/9605104].
- [36] J. Garcia-Bellido, “Open inflation models and gravitational wave anisotropies in the CMB,” Phys. Rev. D **56**, 3225 (1997) [arXiv:astro-ph/9702211].
- [37] A. M. Green and A. R. Liddle, “Open inflationary universes in the induced gravity theory,” Phys. Rev. D **55**, 609 (1997) [arXiv:astro-ph/9607166].
- [38] J. Garriga and V. F. Mukhanov, “On classical anisotropies in models of open inflation,” Phys. Rev. D **56**, 2439 (1997) [arXiv:astro-ph/9702201].
- [39] J. Garcia-Bellido, J. Garriga and X. Montes, “Quasi-open inflation,” Phys. Rev. D **57**, 4669 (1998) [arXiv:hep-ph/9711214].
- [40] J. Garcia-Bellido, “Single-bubble open inflation: An overview,” arXiv:hep-ph/9803270.
- [41] J. Garcia-Bellido, J. Garriga and X. Montes, “Microwave background anisotropies in quasiopen inflation,” Phys. Rev. D **60**, 083501 (1999) [arXiv:hep-ph/9812533].
- [42] R. Kallosh and A. Linde, “Landscape, the scale of SUSY breaking, and inflation,” JHEP **0412**, 004 (2004) [arXiv:hep-th/0411011].
- [43] K. Tomita, Prog. Theor. Phys. **68**, 310 (1982)
- [44] H. Kodama and M. Sasaki, Prog. Theor. Phys. Suppl. **78**, 1 (1984)
- [45] C. R. Contaldi, M. Peloso, L. Kofman, A. D. Linde, “Suppressing the lower multipoles in the CMB anisotropies,” JCAP **0307**, 002 (2003). [astro-ph/0303636].
- [46] L. Susskind, *private communication*